

Modeling and Experimental Verification of an Intermittent Stator Ground Fault Protection Based on a Subharmonic Current Differential Scheme

Nader Safari-Shad, *Senior Member, IEEE*, Adama Sawadogo, James Jensen, and Robert Fecht

Electrical and Computer Engineering Department

University of Wisconsin-Platteville

1680 Green Wood Ave. - Busby Hall

Platteville, WI 53818, USA

safarish@uwplatt.edu

sawadogoa@uwplatt.edu

jensenjam@uwplatt.edu

fechtr@uwplatt.edu

Abstract—The paper highlights the importance of detecting intermittent stator ground faults in large MVA synchronous generators. The detection of such faults can pose a serious challenge to the conventional and some newly proposed IEEE protection schemes. In response to this challenge, an intermittent stator ground fault protection method called the subharmonic current differential scheme (87S) is presented. The efficacy of the 87S scheme is verified by simulation and lab testing using a manufactured apparatus containing all the components of the neutral grounding circuit of large MVA generators which apply the subharmonic voltage injection methodology. The proposed scheme protects the generator stator against intermittent ground faults during online or offline operations.

Index Terms—Generator stator ground fault protection, Fundamental neutral ground overvoltage (59N), Third-harmonic voltage (27TN and 59THD), and subharmonic voltage injection (64S) schemes.

I. INTRODUCTION

A large portion of all power provided to residential and industrial sectors in the US is still supplied by large MVA synchronous generators. These generators are multi-million-dollar assets and they are considered as critical national security infrastructure.

Stator intermittent ground faults (IGF), also known as arcing faults, can occur due to dirty insulators or broken strands in generator stator windings [1]. Due to fast transient overvoltages and intermittent high transient currents which cause heavy iron burning and insulation damages, it is imperative to detect stator IGF before they result in solid (i.e., permanent) ground faults leading to costly repairs and long generator downtimes [2] - [6].

Reports of stator IGF have sparked a renewed interest to detect such faults at their inception [1], [7], [8]. Early research on IGF detection can be traced back to [9] where radio frequency

The authors would like to express their gratitude to WiSys.org for funding this research project under grant numbers T230014 and T240028.

spectrum analysis of neutral grounding current is applied for IGF detection. A more recent study employing a subharmonic voltage injection scheme (64S) is shown to be sufficiently sensitive to detect stator IGF in hydro-generator units provided two additional current transformers (CTs) are used in the neutral grounding circuit [10]. Despite their promising application, however, neither scheme has been implemented in existing commercial generator protective relays [11] - [15].

At present, detection of stator IGF in large MVA generators using IEEE recommended protection schemes 59N, 27TN, 59THD, and 64S is particularly difficult since these schemes are time-delayed [16]. As a result, any single fault may not last long enough to operate the time delayed protective elements. To mitigate this drawback, the use of improved timer schemes such as stall and integrating timers have been proposed [1]. However, the critical assumption in all the improved timer schemes is that at least one of the IEEE recommended protection schemes asserts when stator IGF occur. Unfortunately, this assumption does not always hold for the 59N, 27TN, and 59THD schemes. Specifically, the assumption is invalid when the following conditions hold simultaneously:

- i) The IGF occur in the vicinity of generator neutral where the 59N scheme has a blind zone;
- ii) The 27TN has not been set due to the generator low third-harmonic neutral voltage levels;
- iii) The 59THD has not been set due to generator low third-harmonic voltage levels or generator terminal voltage transformers (VTs) being connected in delta configuration.

It turns out that i) - iii) are not unrealistic scenarios. Specifically, stator IGF occurring near or at the generator neutral are not uncommon [8]. Additionally, there are generators with low third-harmonic neutral voltage levels or where terminal VTs are connected in delta configuration [17]. Moreover, even if ii) and iii) are not the case, setting 27TN and 59THD

are difficult as they require comprehensive generator third-harmonic voltage testing to ensure secure operation. Due to many logistical issues and high cost, often comprehensive testing is practically impossible, leaving the possibility of misoperations [18].

In view of these limitations, the 64S scheme remains as the most viable option for detecting stator IGF. However, the recent simulation-based analysis in [19] has revealed a potential vulnerability of the 64S scheme for detecting stator IGF occurring near or at the generator neutral. The primary goal of the present paper is to delineate this vulnerability by means of stator IGF simulation and experimental lab testing whereby the performance characteristics of the 64S scheme are compared with a newly developed subharmonic current differential scheme called the 87S [19]. To meet this goal, the operating theory of both schemes is briefly reviewed. Then, a complete simulation as well as experimental model of the neutral grounding circuit of large MVA generators are developed and both schemes' performance characteristics are compared by staging stator IGF at or near the generator neutral. The key feature of experimental lab testing is the ability to stage stator IGF safely in a controlled manner without the need for an actual large MVA generator.

II. OPERATIONAL THEORY OF THE 64S SCHEME

Operational theory of the 64S scheme and its variants are reviewed in [20] where the scheme is implemented as shown in Fig. 1. Here, we mainly focus on the overcurrent-based 64S scheme where the neutral grounding current I_{NT} is used for ground fault detection [11].

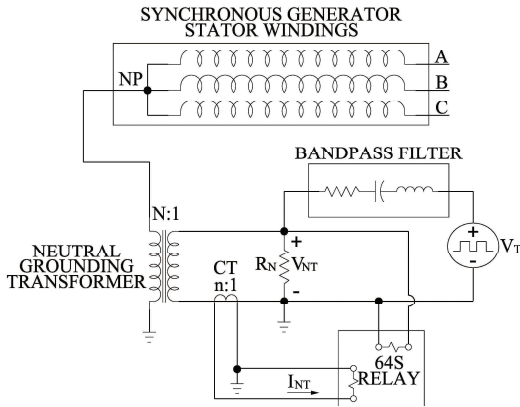


Fig. 1. 64S implementation in large MVA generators

In Fig. 1, V_T is the injection voltage source, R_N is the neutral grounding resistor (NGR), V_{NT} is total neutral voltage across R_N , I_{NT} is the total secondary neutral grounding current, N is the grounding transformer voltage ratio, n is the grounding CT ratio, and NP represents the generator neutral point.

To utilize the overcurrent-based 64S scheme for detection of solid stator ground faults, the equivalent circuit model shown in Fig. 2 is used where V_s , V_N , and I_N are the subharmonic component of V_T , V_{NT} , and I_{NT} , respectively.

Moreover, R_{BPF} is the bandpass filter resistance, R_L is the cable resistance from bandpass filter to NGR, R_S is the healthy stator insulation resistance, and C_0 is the total capacitance to ground of the generator stator windings, iso-phase bus work and delta-connected windings of the step-up transformer. Lastly, R_F is the ground fault resistance.

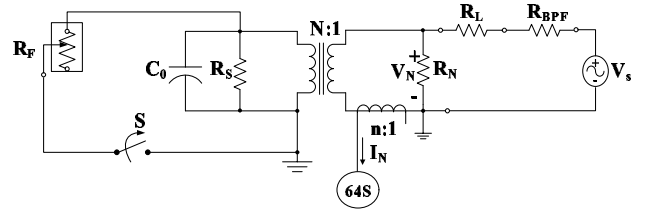


Fig. 2. 64S equivalent circuit model

For solid ground fault detection analysis, the equivalent circuit model in Fig. 2 is used where it is assumed that the switch S closes at the inception of a ground fault and remains closed [21] - [25]. The overcurrent-based 64S operation in [11] is based on two levels where the pickup value for the first level is set based on the magnitude of I_N according to

$$\max |I_N^h| < |I_N|_{pu} < \min |I_N^f| \quad (1)$$

Here, $\max |I_N^h|$ and $\min |I_N^f|$ are, respectively, the maximum healthy and the minimum faulty magnitudes of I_N obtained using generator test data and equivalent circuit model calculations. Similarly, the pickup value for the second level is set based on the real-part of I_N according to

$$\max \operatorname{Re}[I_N^h] < \operatorname{Re}[I_N]_{pu} < \min \operatorname{Re}[I_N^f]. \quad (2)$$

Level 1 provides 100% stator windings ground protection for generators with C_0 less than $1 \mu F$ but has low sensitivity for larger than $1 \mu F$ C_0 cases [24]. Hence, to maintain fault detection sensitivity, both levels are used with the caveat that level 2 is blocked for faults occurring near or at the generator neutral point [24]. This weakness of level 2 is a consequence of the fact that the calculation of $\operatorname{Re}[I_N]$ requires the phase-angle difference between V_N and I_N [11]. However, faults near or at generator neutral point result in small V_N making its phase-angle calculation unreliable.

For intermittent ground fault detection analysis, the switch S must operate intermittently. This is done in [19] where the vulnerability of the 64S scheme for stator IGF near the generator neutral point is shown. Specifically, healthy and faulty magnitudes of I_N captured during testing a 618 MVA generator are used in an idealized switching simulation model. One of the goals of the present paper is to introduce a power electronic circuit by which stator IGF can be staged numerically as well as experimentally.

III. OPERATIONAL THEORY OF THE 87S SCHEME

The 87S scheme was introduced in [19] and its performance was verified using a restricted switching simulation model. Here, we briefly review its operational theory and demonstrate

its performance using a more realistic switching simulation model as well as experimental lab testing.

To present the 87S scheme, we consider the harmonic characteristics of the signal I_{NT} during stator IGF, i.e., the presence of intermittent high transients. These transients can be used as the key signature of stator IGF as it was done in [9]. However, in contrast to [9] which uses intermittent high transients far beyond the power frequency in generator neutral grounding circuits without a subharmonic voltage injection system, here, we use intermittent high transients beyond the subharmonic frequency in generator neutral grounding circuits which employ a subharmonic voltage injection system [21]. It must also be noted that in addition to the intermittent high transients beyond the subharmonic frequency, I_{NT} contains power frequency, third-harmonics, and random measurement noise as well as subharmonic frequency contents. Therefore, stator IGF detection is viewed as a filtering problem where intermittent high transients beyond the subharmonic frequency in I_{NT} must be extracted and used for fault detection.

To design appropriate filters for this extraction, we let $\Delta(t)$ denote a *subharmonic current differential operate signal*, i.e.,

$$\Delta(t) = \mathcal{H}(I_{NT}(t)) \quad (3)$$

where the linear operator \mathcal{H} is expressed as the difference of two linear operators, i.e.,

$$\mathcal{H} = \mathcal{H}_1 - \mathcal{H}_2 \quad (4)$$

The operators in (4) are realized by linear time-invariant (LTI) filters [26]. Specifically, \mathcal{H}_1 is realized by a cascade of three filters consisting of a lowpass filter in series with two notch filters, i.e.,

$$H_1(s) = H_{lo}(s) H_{no1}(s) H_{no2}(s) \quad (5)$$

where

$$H_{lo}(s) = \frac{2.527 \times 10^9}{s^2 + 9.048 \times 10^4 s + 2.527 \times 10^9} \quad (6)$$

$$H_{no1}(s) = \frac{s^2 + 1.421 \times 10^5}{s^2 + 75.4s + 1.421 \times 10^5} \quad (7)$$

$$H_{no2}(s) = \frac{s^2 + 1.279 \times 10^6}{s^2 + 226.2s + 1.279 \times 10^6} \quad (8)$$

Note that H_{lo} is designed to filter out the random measurement noise in I_{NT} and has a bandwidth of approximately 6 kHz while H_{no1} and H_{no2} are designed with a narrow stop-band to block the 60 Hz power frequency and possible 180 Hz contents in I_{NT} , respectively.

To complete the operational theory of the 87S scheme, we now define a *subharmonic restraint signal* denoted $\epsilon(t)$, i.e.,

$$\epsilon(t) = \mathcal{H}_2(I_{NT}(t)) \quad (9)$$

Here, the \mathcal{H}_2 operator is realized by a bandpass filter with a center frequency of 20 Hz (subharmonic frequency), i.e.,

$$H_{bpf}(s) = \frac{13.19s}{s^2 + 13.19s + 1.579 \times 10^4} \quad (10)$$

Hence, the signal produced by the \mathcal{H}_2 operator will be at the subharmonic frequency during the healthy and stator IGF.

Using (3) and (9), alarm and trip logics can be defined according to

$$\begin{aligned} \text{Alarm if: } & \mathcal{P}(\Delta(t)) > \beta_a \mathcal{P}(\epsilon(t)) \quad \text{for } t \in \{t_1, \dots, t_k\} \\ \text{Trip if: } & \mathcal{P}(\Delta(t)) > \beta_t \mathcal{P}(\epsilon(t)) \quad \text{for } t \in \{t_1, \dots, t_j\} \end{aligned} \quad (11)$$

where $\mathcal{P}(\cdot)$ denotes the *peak-value operator*, and β_a , β_t are fixed user specified alarm and trip sensitivity factors, respectively. Moreover, t_i 's are time instances when operate quantity exceeds the restraint quantity in each case. Finally, two counters are used to enable alarm and trip logics with user specified pickups.

In the next section, we present a stator IGF model whereby the performance of the 64S and 87S schemes are compared.

IV. SIMULATION-BASED PERFORMANCE COMPARISON

In this section, an IGF model is developed for comparing the responses of the overcurrent-based 64S and the proposed 87S schemes. The model is developed based on Fig. 1 which depicts all the electrical components used in the neutral grounding circuit of typical large MVA generators when the 64S element is implemented for stator ground protection. These electrical components are all available in the *Simscape toolbox* of Matlab/Simulink and can be used to construct a simulation model for IGF staging and fault detection comparison. The constructed model is shown in Fig. 3.

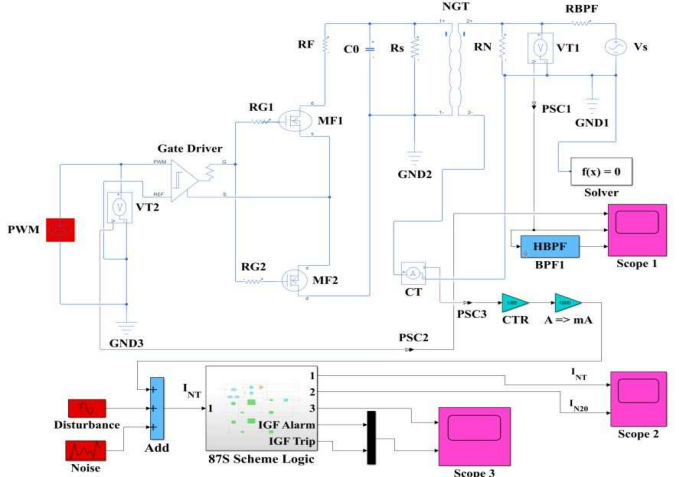


Fig. 3. Simulink model of the generator neutral grounding circuit with the added 87S scheme logic

A key feature of the model is the inclusion of two power MOSFETs labeled MF1 and MF2 along with their gate resistors RG1 and RG2, to emulate the IGF switching action. Specifically, both MOSFETs are controlled by a gate driver integrated circuit (GDIC) whose input is a PWM signal with selectable frequency. The two MOSFETs along with the GDIC realize a four-quadrant AC switch [30] that emulates the intermittent switching of S in Fig. 2.

The model uses a 20 Hz injection source V_s and incorporates two classes of input disturbances, i.e., a power current disturbance for when the generator is online and a random disturbance for measurement noise. Moreover, the model includes the 87S scheme logic inside the *masked block* with the required LTI filters, peak detectors, comparators, alarm/trip counters, and necessary time delays. In particular, the 20 Hz bandpass, lowpass and notch filters are realized by the transfer functions given in (6) - (10). An initial time delay unit is used to disable the 87S alarm/trip logic for a period of 0.5 seconds. This ensures that the element does not operate due to startup transients. The alarm and trip counter pickups are set to 10 and 30 counts, respectively. The alarm and trip counters are reset if stator IGF cease for 5 sampling instances after having recorded 5 and 15 counts, respectively.

To have a realistic model, the neutral grounding circuit parameters are taken from the 618 MVA generator given in [22]. The complete list of the IGF simulation and neutral grounding circuit parameters are given in Table I.

The stator IGF simulations are carried out by capturing the I_{NT} signal during a 2.5 second interval where the AC switch in Fig. 2 is open rendering the healthy data, i.e., I_{NT}^h and its 20 Hz component I_{N20}^h . This is followed by a second stage consisting also of a 2.5-second interval where the AC switch is intermittently operated rendering the faulty data, i.e., I_{NT}^f and its 20 Hz component I_{N20}^f . The switching action is actuated by setting the PWM signal frequency at 120 Hz. The rationale behind the 120 Hz frequency comes from the fact that stator IGF typically start at the generator faulted phase voltage peak each half cycle and extinguish at the generator fault current zero [3], [4]. With this assumption, the percentage ratio of on-time to period of the PWM signal, called the duty cycle D, can be varied to stage stator IGF at various stator winding locations, i.e., small values of D correspond to shorter duration stator IGF which in [1] and [5] are shown to correspond to IGF occurring near stator windings neutral while large values of D correspond to longer duration IGF occurring near stator windings terminal. Given that the blind zone of the 59N scheme is near the generator neutral point, we are naturally more concerned with smaller duty cycle IGF.

TABLE I
64S/87S SIMULATION MODEL PARAMETERS

Parameter	Numerical value
20 Hz injection source amplitude (V)	42.5
Neutral grounding CT ratio n	425:5
Neutral grounding transformer ratio N	60:1
Neutral grounding resistor $R_N(\Omega)$	0.35
Stator insulation resistance $R_S(\Omega)$	100 k
Fault resistor $R_F(\Omega)$	0, 10, 100, 1k, 5k, 10k, ∞
Gate resistors $R_{G1} = R_{G2}(\Omega)$	47
Total coupling capacitance $C_0(\mu F)$	0.78
Power current disturbance (A)	0.5
Measurement noise (A)	[−0.01, 0.01]
87S sensitivity factors $\beta_{a/t}$	0.35

Figures 4 - 9 display plots of the stator IGF simulation starting with the total secondary neutral current I_{NT} , its 20 Hz component I_{N20} , the 87S operate and restraint quantities, $\Delta(t)$, $\beta_{a/t} \epsilon(t)$, respectively. The figures show the responses of the two schemes to simulated IGF for D = 5%, 10%, and 50%, respectively. In all the simulations, the alarm and trip sensitivity factors $\beta_{a/t}$ are set to 0.35 while the fault resistor R_F is set to 1 kΩ.

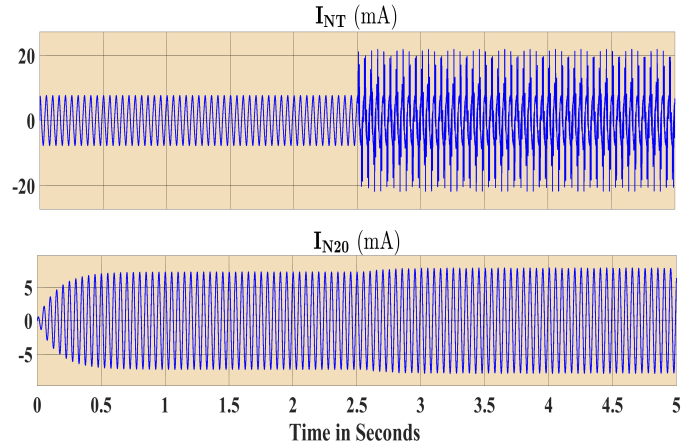


Fig. 4. Pre-fault and post-fault neutral currents for D = 5%

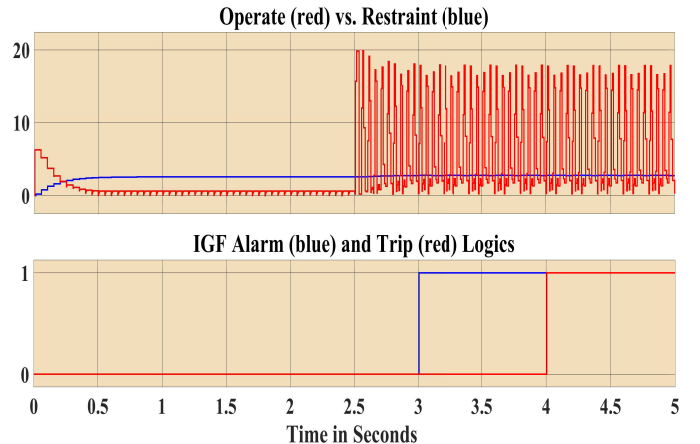


Fig. 5. IGF responses of 87S scheme for D = 5%

Inspecting the simulated responses, it is clear that the conventional overcurrent-based 64S scheme is unable to detect the simulated IGF near the generator neutral point. This can be seen by the fact that the amplitude of I_{N20} from pre-fault to post-fault does not change significantly at smaller duty cycles. On the other hand, as the duty cycle increases, i.e., the IGF occur away from the generator neutral point, the conventional overcurrent-based 64S scheme regains its sensitivity.

Next, we show that IGF near the generator neutral point pose an even bigger challenge to the conventional overcurrent-based 64S scheme as the fault resistance R_F increases. To do this, the corresponding simulation results for $\beta_{a/t} = 0.35$ and

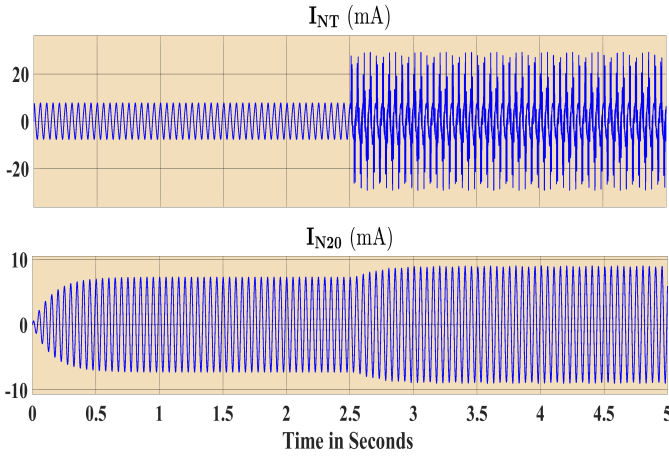


Fig. 6. Pre-fault and post-fault neutral currents for $D = 10\%$

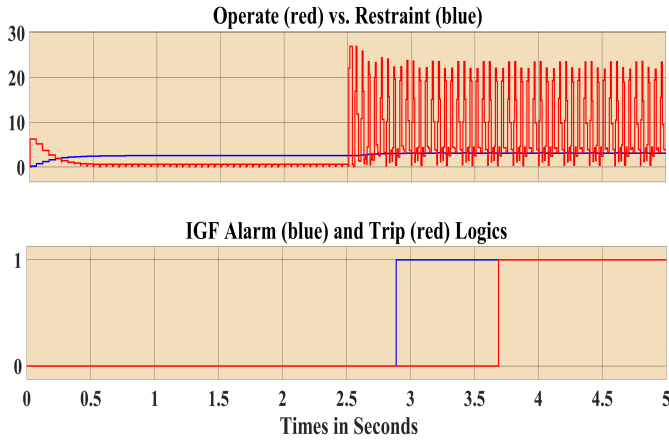


Fig. 7. IGF responses of 87S scheme for $D = 10\%$

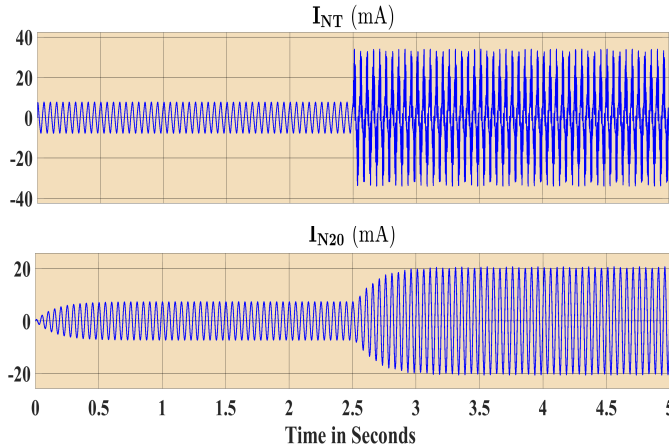


Fig. 8. Pre-fault and post-fault neutral currents for $D = 50\%$

$R_F = 5 k\Omega$ are shown in Figures 10 and 11 for $D = 10\%$. Fig. 10 clearly shows that the amplitude of I_{N20} does not change at or after the inception of the IGF making it impossible for the 64S scheme to detect the fault. On the other hand,

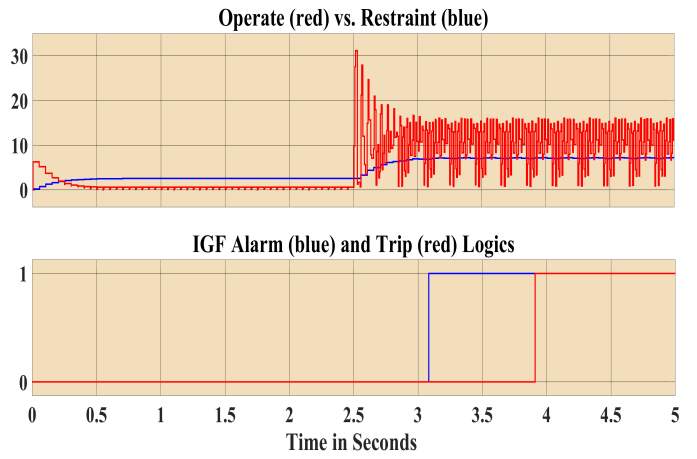


Fig. 9. IGF responses of 87S scheme for $D = 50\%$

Fig. 11 clearly shows that both 87S alarm and trip assert.

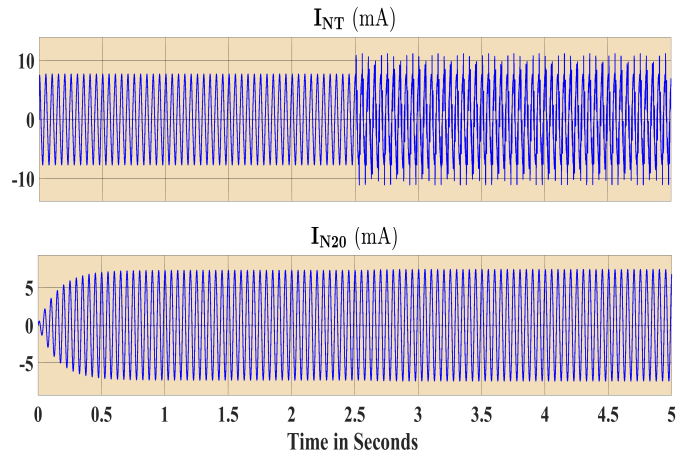


Fig. 10. Pre-fault and post-fault neutral currents for $D = 10\%$

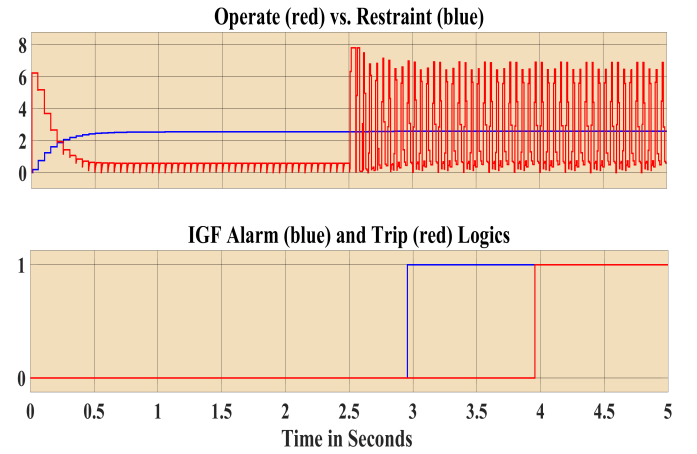


Fig. 11. IGF responses of 87S scheme for $D = 10\%$

In the next section, we describe how a lab testing apparatus

for experimental performance verification of the two schemes can be constructed.

V. IGF EXPERIMENTAL LAB TESTING APPARATUS

To construct a lab testing apparatus whereby the 64S and 87S schemes' performance can be compared experimentally, all physical devices and equipment in Fig. 1 are required. The use of a large MVA generator in such an apparatus would of course be impossible due to many safety as well as logistical issues. While the use of a small generator is certainly a possibility, our past experience has shown that the experimental results do not readily scale up to large MVA generators due to extremely low C_0 value of small generators [27].

Fortunately, the literature on the 64S stator ground protection element suggests that the equivalent circuit model of a large MVA generator is sufficient to perform setting calculations [10], [21] - [25]. For this reason, the equivalent circuit model in Fig. 2 is used for stator IGF lab testing and performance comparison of the two schemes.

Table II lists the specifications of all the needed equipment for constructing a lab testing apparatus. Note that the Flex-Core CTWH3-60-T50 [28] is the Beckwith recommended CT for the 64S application [11]. However, due to its low bandwidth (BW), the GMW Magnelab CT [29] is used here in addition to the Flex-Core CT. The GMW Magnelab CT has a much wider bandwidth making it ideal for the 87S application.

Figures 12 and 13 show the wiring diagram along with the physical construction of major components of the lab testing apparatus.

TABLE II
IGF EXPERIMENTAL LAB TESTING PARAMETERS

Equipment	Specification
Beckwith M3425A generator relay	With the 64S element
Siemens 7XT33	20 Hz signal generator
Siemens 7XT34	20 Hz bandpass filter
Neutral grounding GMW CT (CT1)	10 A/V, BW = 50 MHz
Neutral grounding Flex-Core CT (CT2)	425:5, BW = 400 Hz
Neutral grounding voltage transformer	25 kVA with 60:1 ratio
Fault resistor $R_F(\Omega)$	0, 10, 100, 1k, 5k, 10k, ∞
Neutral grounding resistor $R_N(\Omega)$	0.5 (2 1.0 Ω in parallel)
Stator insulation resistance $R_S(\Omega)$	100 k
Total coupling capacitance $C_0(\mu F)$	0.5 (2 1.0 μF in series)
Gate switch resistors $RG1 = RG2(\Omega)$	47
Microcontroller	Arduino Uno 3.0

The remaining components of the lab testing apparatus are mounted in an enclosure. The enclosure yields a 64S/87S *test instrument* which performs solid and intermittent ground fault staging with user specified fault resistance and has data acquisition capability. Fig. 14 shows the interior and exterior of the test instrument.

VI. IGF EXPERIMENTAL DATA ACQUISITION

We are now ready to present a procedure for staging stator IGF experiments and capturing the required data. Specifically,

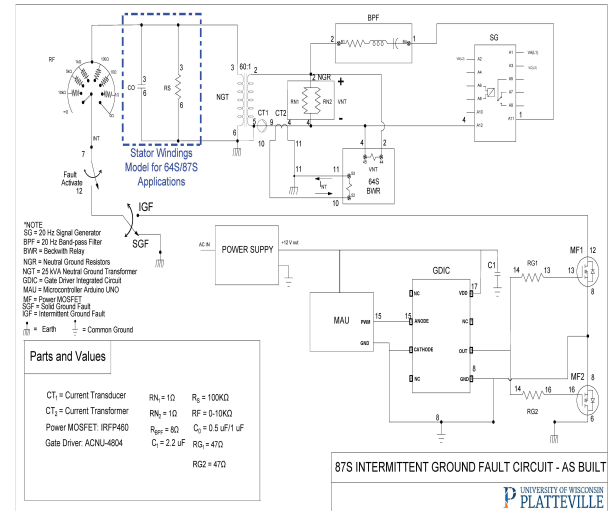


Fig. 12. Wiring diagram of the overall lab testing apparatus

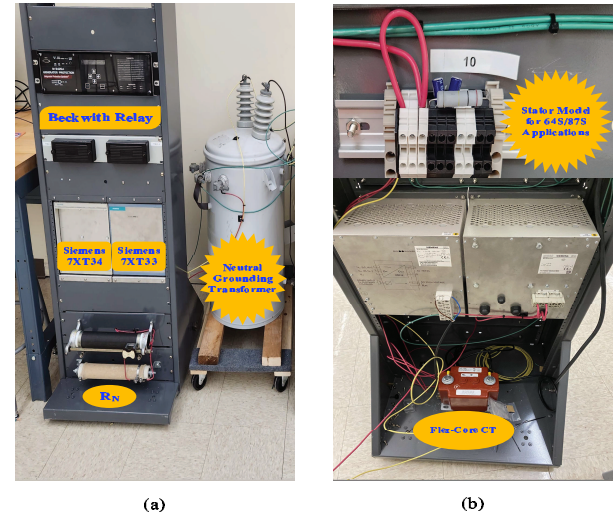


Fig. 13. Testing apparatus - (a) front view, (b) rear view



Fig. 14. 64S/87S test instrument - (a) interior view, (b) exterior view

the stator IGF experiments are carried out by capturing the I_{NT} signal during a 2.5-second interval where the four-quadrant AC switch shown in Fig. 12 is open rendering the generator model healthy data. Then, a second experimental stage consisting also of a 2.5-second interval is carried out where the four-quadrant

AC switch is intermittently operated. Similar to the staged stator IGF simulations, this action is actuated by injecting a PWM signal with a fundamental frequency of 120 Hz and duty cycle D. Finally, a 5-second long I_{NT} data is obtained by stitching the two 2.5-second long data sets.

The I_{NT} signal during each 2.5-second interval is measured using CT1. Specifically, the output of CT1 which is a voltage proportional to I_{NT} is captured at a sampling rate of 1 msec using a digital storage oscilloscope. The captured voltage signal is then converted to primary amps using the 10 A/V conversion factor. Finally, to evaluate and compare the efficacy of the 87S detection scheme with that of the 64S, I_{NT} is divided by the CT2 ratio to obtain the secondary amps that the Beckwith M3425A relay measures. Fig. 15 shows how the experimental data is processed in Simulink after performing all the required conversions.

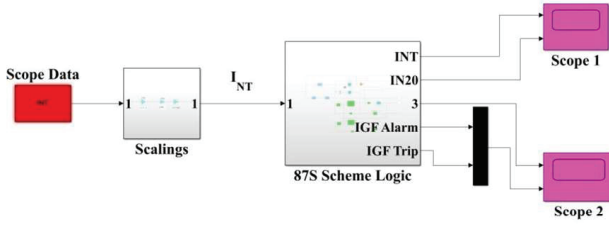


Fig. 15. Simulink block diagram for processing the experimental data

The subsystems of the masked block in Fig. 15 are identical to those shown in Fig. 3.

VII. IGF EXPERIMENTAL DATA ANALYSIS

This section reports on the analysis of captured experimental data and performance comparison of the 64S and 87S schemes. Specifically, the experimental lab testing apparatus in Fig. 13 is used to generate a variety of stator IGF data when the generator's total capacitance to ground is $C_0 = 0.5 \mu F$ and the fault resistance $R_F = 1 k\Omega$. The experiments are run for the duty cycles $D = 5\%, 10\%$ and 50% representing stator IGF occurrence near the generator neutral and further towards the middle of the generator stator windings, respectively.

Figures 16 - 21 display the plots of the stator IGF experimental data starting with the total secondary neutral current I_{NT} , its 20 Hz component I_{N20} , the 87S operate $\Delta(t)$ and the restraint $\beta_{a/t} \epsilon(t)$ quantities, respectively. The sensitivity setting $\beta_{a/t}$ for all the cases is set at 0.35 to ensure the scheme is secure during the healthy portion as well as being sufficiently sensitive during the stator IGF portion.

The critical observation in Figures 16 - 21 is that at low values of D, the change in I_{N20} from a healthy state to a faulty state is insignificant. Specifically, only when $D = 50\%$ that the change in I_{N20} from a healthy state to a faulty state becomes significant. Hence, the overcurrent-based 64S scheme cannot be set to reliably detect stator IGF near the generator neutral point. Given that the conventional IEEE recommended 59N scheme has a blind zone near the generator neutral point,

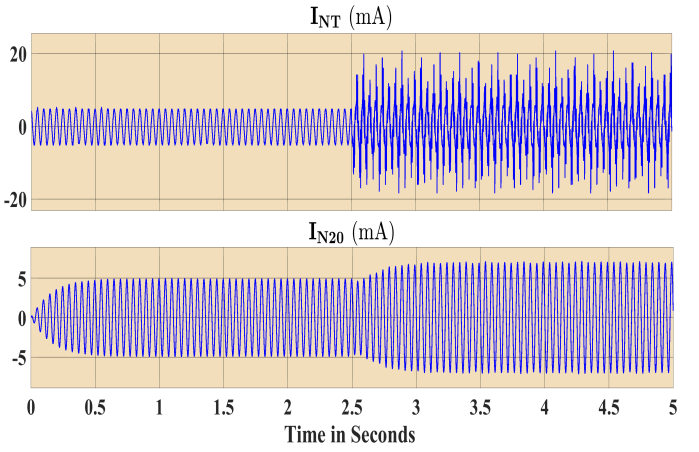


Fig. 16. Pre-fault and post-fault neutral currents for $D = 5\%$

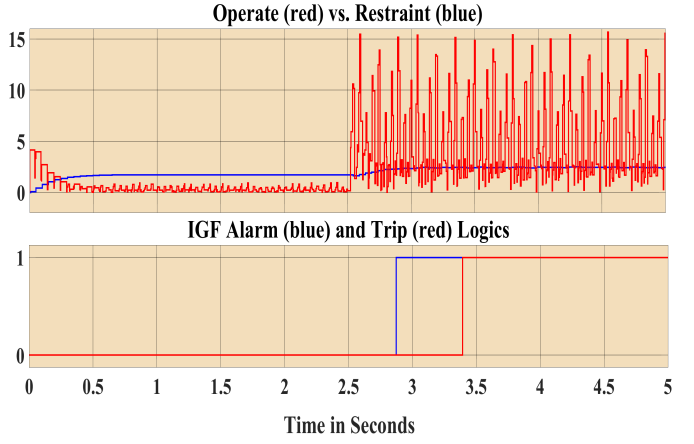


Fig. 17. IGF responses of the 87S scheme for $D = 5\%$

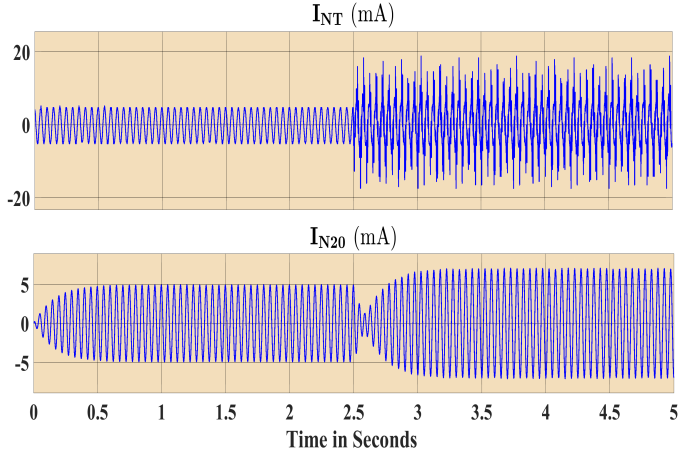


Fig. 18. Pre-fault and post-fault neutral currents for $D = 10\%$

using a 64S and 59N to attain 100% stator intermittent ground fault protection will not be realized.

Finally, it is well-known that the overcurrent-based 64S scheme has reduced sensitivity when the generator total cou-

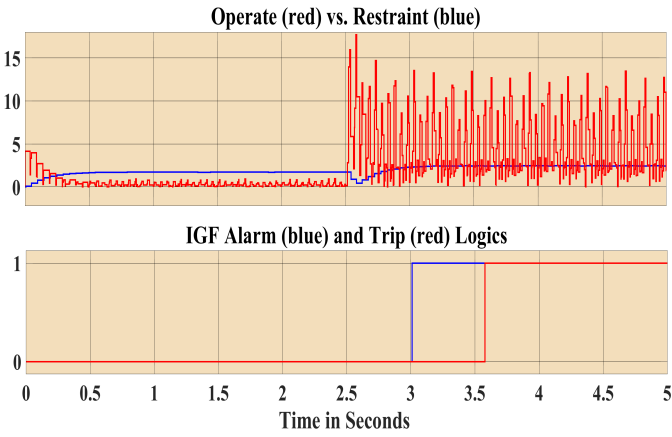


Fig. 19. IGF responses of the 87S scheme for $D = 10\%$

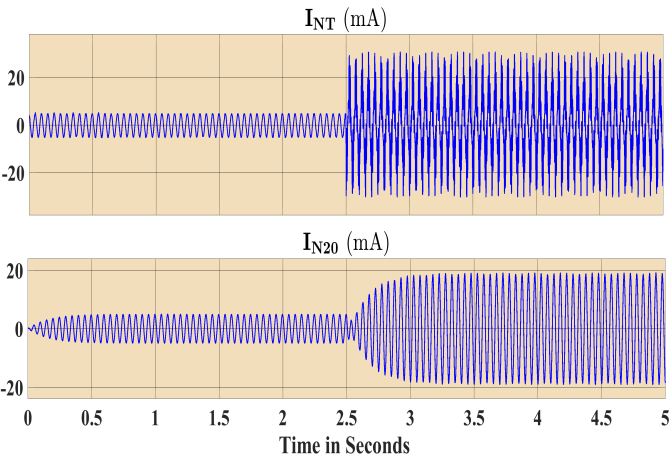


Fig. 20. Pre-fault and post-fault neutral currents for $D = 50\%$

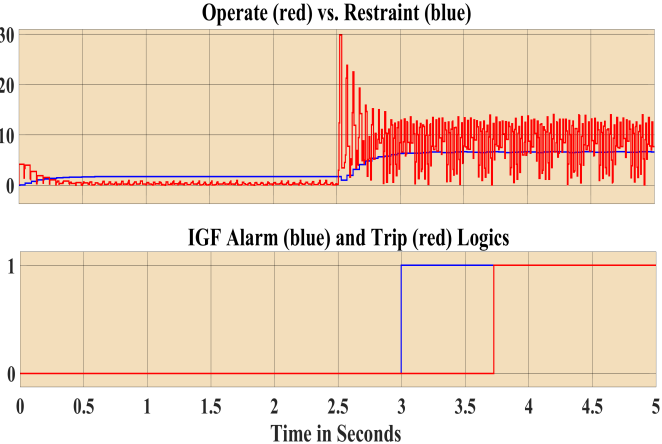


Fig. 21. IGF responses of the 87S scheme for $D = 50\%$

pling capacitance is relatively large (e.g., in the case of hydro-generators) [10]. To demonstrate that the 87S scheme maintains its sensitivity even for generators with large C_0 , an experiment is conducted using $C_0 = 1.0 \mu F$, $R_F = 1 k\Omega$ when

$D = 10\%$. Fig. 22 shows the resulting graphs of I_{NT} and I_{N20} where once again the change from healthy state to faulty state in I_{N20} is observed to be insignificant while in Fig. 23 the corresponding operate and restraint quantities show that the 87S alarm and trip logics operate using the same sensitivity factor $\beta_{a/t} = 0.35$.

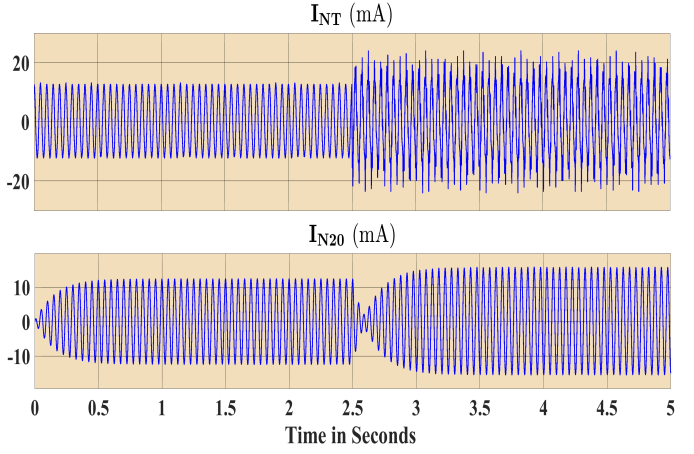


Fig. 22. Pre-fault and post-fault neutral currents for $D = 10\%$

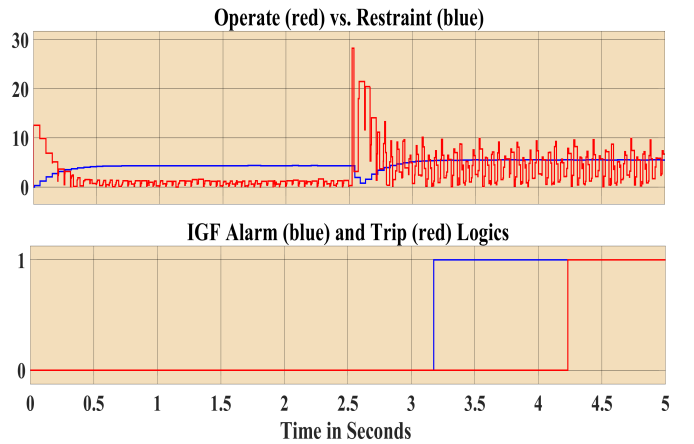


Fig. 23. IGF responses of 87S scheme for $D = 10\%$

VIII. CONCLUSION

The paper delineates vulnerability of the conventional and some newly proposed IEEE protection schemes for detecting stator IGF at or near the neutral point of large MVA generators. This is particularly concerning since the conventional IEEE recommended 59N scheme has a blind zone near the generator neutral point. This implies that a combination of 59N and 64S schemes, contrary to the suggestion in [1], will not provide reliable stator IGF protection. To overcome this issue, the paper proposes a subharmonic current differential scheme (87S) whose efficacy for reliable stator IGF detection is verified using simulation and experimentation. The lab testing apparatus constructed for the experimental verification allows

performing controlled solid and intermittent stator ground fault experiments without the need for an actual large MVA generator. The experimental verification process results in devising a test instrument which is interesting in its own right. Specifically, the manufactured test instrument serves as a valuable device for generating solid and intermittent ground fault data with low or high fault resistance. As such, the instrument can be used for staging both types of faults during relay commissioning of *actual* large MVA generators which employ the subharmonic voltage injection methodology.

Since the success of the proposed 87S scheme hinges on detecting intermittent high-frequency current transients, the neutral grounding CT must have a sufficiently large bandwidth. This requirement is easily satisfied by using reasonably priced commercial CTs capable of measuring currents from microamps maximum peak, at frequencies ranging from 2 Hz to 50 MHz [29]. Moreover, the proposed 87S scheme can be readily implemented in existing 64S commercial microprocessor relays [11] - [15] through a mere firmware upgrade.

As for future research, it is believed that the experimental staging of intermittent ground faults presented in this paper can be modified to analyze detection of hazardous high-impedance faults in power distribution networks [31].

REFERENCES

- [1] IEEE Power System Relaying and Control Committee (PSRC) J12 Subcommittee Technical Report, "Improved Generator Ground Fault Schemes," *PES-TR82*, Sept. 1, 2020.
- [2] J. R. Dunki-Jacobs, "The Escalating Arcing Ground-Fault Phenomenon," *IEEE Trans. on Industry Applications*, Vol. IA-2225, no. 6, pp 1156-1161, Nov/Dec, 1986.
- [3] M. Fulczyk, W. Piascicki, and J. Bertsch, "Fast Transient Overvoltages in Generator Stator Windings during Interrupted Arcing Ground-Faults," *IEEE Porto Power Tech. Conf.*, Porto, Portugal, Sept. 2001.
- [4] D. Braun and G. S. Koeppl, "Intermittent Line-to-Ground Faults in Generator Stator Windings and Consequences on Neutral Grounding," *IEEE Trans. on Power Del.*, Vol. 25, no. 2, pp 876-881, Apr. 2010.
- [5] G. S. Koeppl, and D. Braun, "New Aspects for Neutral Grounding of Generators Considering Intermittent Faults," *CIDEL Argentinak*, Sept. 2010.
- [6] C. V. Maughan, "Stator Winding Ground Protection Failures," Proc. of the ASME Power Conf., July 2013.
- [7] Sosa-Aguiluz, M., Guzman, A., Eternal, J. L., "CFE Generator Protection Guidelines for Setting 40 and 64G schemes Based on Simulations and Field Experience," *68th Annual Conference for Protective Relay Engineers*, College Station, TX, pp. 389-404, 2015.
- [8] N. Klingerman, L. Wright, B. Cockerham, "Field Experience with Detecting an Arcing Ground Fault on a Generator Neutral Point," 42nd Annual Western Protective Relay Conference, October 2015.
- [9] F.T. Emery, and R.T. Harrold, "On Line Incipient Arc Detection in Large Turbine Generator Stator Windings," *IEEE Trans. on Power Apparatus and Systems*, Vol. PAS-99, No. 6 Nov/Dec 1980.
- [10] J. Wu, H. Wan, and Y. Lu, "Study of a Fresh Subharmonic Injection Scheme Based on Equilibrium Principle for Hydro-Generator Stator Ground Protection," *IEEE PES Winter Meeting*, Vol. 2, pp. 924-929, 2002.
- [11] "Beckwith Electric, M3425A Generator Protection Relay Instructional Book," Beckwith Electric Inc. Publication.
- [12] "SEL-400G Advanced Generator Protection System," Instructional Manual, Schweitzer Engineering Laboratories, date code 20200518.
- [13] "Schneider Electric MiCOM P345 Generator Protection," Relay Technical Manual, 2010.
- [14] "ABB Inc. Generator Protection REG670 Application Manual," Document ID: 1MRK 502 030-UEN, Revision B, Dec. 2012.
- [15] "GE Digital, GPM Field and Stator Ground Fault Protection Modules," GE publication code: 1601-0256-Z1 (GEK-113231B), Feb. 2013.
- [16] IEEE Std. C37.102-2006, IEEE Guide for AC Generator Protection, IEEE PES publication.
- [17] N. Safari-Shad and R. Franklin, "Achieving Reliable Generator 100% Stator Ground Fault Protection," *74th Annual Conf. for Protective Relay Engineers*, College Station, TX, March 2021.
- [18] N. Safari-Shad and R. Franklin, "Adaptive 100% Stator Ground Fault Protection Based on Third-Harmonic Differential Voltage Scheme," *IEEE Trans. on Power Del.*, Vol. 31, No. 4, pp. 1429-1436, Sept. 26, 2015.
- [19] N. Safari-Shad and R. Franklin, "Stator Intermittent Ground Fault Detection in High-Impedance Grounded Generators," *IEEE 32nd International Symposium on Industrial Electronics*, Aalto University, Helsinki-Espoo, Finland, June 19-21, 2023.
- [20] N. Safari-Shad, R. Franklin, A. Negahdari, and H. A. Toliyat, "Adaptive 100% Injection-based Generator Stator Ground Fault Protection with Real-time Fault Location Capability," *IEEE Trans. on Power Del.*, Vol. 33, No. 5, pp 2364-2372, Oct. 2018.
- [21] T. Bengtsson, Z. Gajic, H. Johansson, J. Menezes, S. Roxenborg, and M. Sehlstedt, "Innovative Injection-Based 100% Stator Earth-Fault Protection," *11th IET Conf. on Developments in Power System Protection*, 2012.
- [22] N. Safari-Shad and R. Franklin, "Performance Verification of an Adaptive 100% Injection-Based Stator Ground Fault Protection Using a Large MVA Generator," *72nd Annual Conf. for Protective Relay Engineers*, College Station, TX, March 2019.
- [23] "Beckwith Electric Application Note on 64S 100% Stator Ground Protection," Apr. 2020.
- [24] S. Turner, "Applying 100% stator ground fault protection by low frequency injection for generators," in *Proc. IEEE Power Energy Soc. Gen. Meeting*, pp. 1-6, Jul. 2009.
- [25] R. Preston and J. Kandrac, "Report on Design, Testing and Commissioning of 100% Stator Ground Fault Protection at Dominions Bath County Pumped-Storage Station," in *Proc. IEEE Power System Conf.*, pp. 1-13, 2009.
- [26] B. P. Lathi and R. Green, "Linear Systems and Signals," 3rd ed., New York, Oxford University Press, 2018.
- [27] K. A. Jaafari, A. Negahdari, H. A. Toliyat, N. Safari-Shad, and Russ Franklin, "Modeling and Experimental Verification of a 100% Stator Ground Fault Protection Based on Adaptive Third-Harmonic Differential Voltage Scheme for Synchronous Generators," *IEEE Trans. on Industry Applications*, Vol. 53, No. 4, July/August 2017.
- [28] Flex Core Current Transformer, <https://www.flex-core.com>.
- [29] MagneLab Current Transformer, <https://gmw.com/product/ct/>.
- [30] G. Venkataraman and N. Kogalur, "A Hybrid 4-quadrant Switch for AC Power Conversion," *IEEE Energy Conversion Congress and Exposition*, p. 5487 - 5493, Baltimore, Maryland, Sept. 2019.
- [31] E. Hamatwi et al. "Comparative Analysis of High Impedance Fault Detection Techniques on Distribution Networks," *IEEE Access*, Vol. 11, 2023.